Advances in Research
8(2): 1-21, 2016; Article no.AIR.30019
ISSN: 2348-0394, NLM ID: 101666096

SCIENCEDOMAIN *international*
www.sciencedomain.org

Hybird, Solar and Biomass Energy System for Heating Greenhouse Sweet Coloured Pepper

S. M. Abdellatif[1], N. M. El Ashmawy[2*], M. K. El-Bakhaswan[2] and H. H. Tarabye[3]

[1]Department of Agricultural Engineering, Mansoura University, Mansoura, Egypt.
[2]Agricultural Engineering Research Institute, ARC, Giza, Egypt.
[3]Department of Agricultural Engineering, Aswan University, Aswan, Egypt.

Authors' contributions

This work was carried out in collaboration between all authors. Author SMA designed the study, wrote the protocol, supervised the experimental work and wrote the first draft of the manuscript. Author NMEA collected the data and analyses of the study performed the thermal performance of solar heating system. Author MKEB managed the experimental data of the biomass heat energy and analyses the thermal performance of biomass system. Author HHT managed the literature searches and analyses of the hybrid heating system. All authors read and approved the final manuscript.

Article Information

DOI: 10.9734/AIR/2016/30019
Editor(s):
(1) Prabhakar Tamboli, Director International Training Program, Department of Environmental Science & Technology, University of Maryland, USA.
Reviewers:
(1) Enrique Rico García, Autonomous University of Queretaro, Mexico.
(2) César Ernesto Hernández Hernández, University of Almeria, Spain.
Complete Peer review History: http://www.sciencedomain.org/review-history/16957

Original Research Article

Received 12th October 2016
Accepted 10th November 2016
Published 18th November 2016

ABSTRACT

The main drawback of greenhouse heating systems based on solar energy is the unavailability at nighttime and the variation of its value from hour to hour and month to another during daylight-time. However, use the combination of two-source of renewable energy (solar energy and biomass heat energy) successfully provides appropriate amount of heat energy for heating greenhouse at nighttime. The commercial greenhouses have the highest demand of heat energy for heating the indoor air as compared with other agricultural industry sectors. The investigation presented in this article is aimed at evaluating the technical and design feasibility of using biomass heat energy to assist the solar energy heating system at the eastern area of coastal delta, Egypt (Latitude and longitude are 31.045º N and 31.37º E, respectively, and altitude 6.0 m above the sea level). The hybrid heating system (solar and biomass heating systems) is mainly consists of two different heating systems, a complete solar heating system (6 collectors, storage tank and heat exchanger)

**Corresponding author: E-mail: nalashmawe@ksu.edu.sa;*

and biomass burner (water and air coils, and air heat exchanger). The obtained results reveal that, over 180 days heating season (from November 2015 to March 2016) the solar heating system collected 12712 kWh (45.763 GJ) of which 12316 kWh (44.338 GJ) of solar heat energy was stored in the storage tank. It provided 30.32% of the total heat energy required for heating the greenhouse. The biomass heating system provided 19795 kWh (71.262 GJ) of heat energy which provided 58.55% of the total heat energy required for heating the greenhouse (225.389 kWh). Ultimately, the heat energy provided by the hybrid heating system (88.87%) has been used successfully to heat up the indoor air of the commercial greenhouse sweet coloured pepper.

Keywords: Biomass heat energy; solar energy; hybrid heating system; burden of heating; thermal performance.

1. INTRODUCTION

Vegetable crop production using greenhouses has rapidly increased in Egypt over the last two decades. Protected cropping provides an excellent opportunity to produce high quality fresh yield and assured regular supply in huge quantity. Protected cropping using commercial greenhouse has the highest demand for heat energy to provide optimal indoor environmental conditions. In cold winters, the indoor air temperature of a greenhouse without a heating system can fall below the optimal level for different crops especially at night-times. Therefore, an appropriate heating system is required to provide and maintain the indoor air temperature at desired level [1]. Many greenhouse operations using natural gas as their primary source of heating fuel have used light oil as a secondary source of fuel to provide a backup in case of natural gas supply interruption. In some situations, a gas supply company may request a greenhouse operator switched to an alternate fuel source to increase the availability of natural gas to a residential user during exceptionally cold periods in the winter [2].

Nowadays, the impact of fuel price crisis coupled with the awareness of global heating problem has brought about changes in the structure of energy usage all over the world. Higher importance is now given to research, development, and promotion of renewable energy sources (solar energy, biomass energy, biogas energy, wind energy, and biochemical fuels). These resources have massive energy potential, however, they are generally diffused and not fully accessible, most of them are intermittent, and have distinct regional variability. These characteristics give rise to difficult, but solvable, technical and economical challenges [3].

Thermal solar energy collectors are special kind of heat exchangers that transform solar radiation energy into internal energy of the transport medium. The major component of any solar system is the solar collector which absorbs the incoming solar radiation energy, converts it into thermal energy, and transfers this thermal energy to a fluid (usually water, air, or oil) passes through the collector. The thermal solar energy thus collected is carried from the circulating fluid either directly to the hot water or space conditioning equipment or to a thermal energy storage tank from which can be drawn for use at night-times or cloudy days. The solar collectors are basically distinguished by their motion, i.e. stationary non-tracking, single axis tracking and two axes tracking, and the operating temperature [4,5,6]. The solar collectors should be orientated directly towards the equator, facing south in the northern hemisphere and north in the southern. The optimum tilt angle of the solar collector is almost equal to the latitude angle of the location with angle variations of 10–15º more or less depending on the application [5,7]. The solar collector plate absorbs as much of the irradiation as possible through the glazing, while losing as little heat as possible upward to the atmosphere and downward through the back of the casing. The solar collector plates transfer the retained heat into the transport fluid. The effective absorptance of the absorber plate surface for shortwave solar radiation depends strongly upon the nature and the colour of the coating and on the solar incident angle. Usually black colour of the coating is used, however, various colour coatings have been proposed by several researchers mainly for aesthetic reason [8,9,10,11].

The biomass exploitation takes advantage of the field and livestock residues which under controlled burning conditions, can generate heat energy and electrical power, with limited environmental impacts [12]. The thermal energy applications in space heating and hot water utilities of the modern biomass combustion

systems could meet the contemporary energy requirements with the least possible environmental impacts. The controlled combustion technology has been successfully applied in some European areas, by heating entire city clusters through district heating networks. Moreover, the favourable funding of energy investments in this particular technology makes its implementation attractive [13]. Design of biomass district heating systems, thermal performance, and applications in agricultural sector have been studied and examined by several researchers [3,14,15,16]. However, there is no readily available information about the combination of biomass heat energy and solar energy for providing burden of heating for commercial greenhouses. To insure optimum fruit yields of greenhouse sweet coloured pepper in the eastern area of coastal delta, Egypt, during winter growing season when greenhouse night temperatures can be in lower of 10ºC, burden of heating should be added to the greenhouse. Therefore, the aim of the present study was to evaluate the thermal performance of hybrid heating system includes combination of biomass and solar heating systems for heating commercial greenhouse sweet pepper during winter season.

2. MATERIALS AND METHODS

2.1 Greenhouse Position and Equipment

The experimental work was carried out during winter season of 2015/2016 (from November 2015 to March 2016) in a commercial controlled gable-even-span greenhouse, east-west orientated in a site free from shading by surrounding buildings and trees, at the Agricultural Research Centre of Mansoura University. The greenhouse has a geometrical characteristics of; total length 30.8 m, total width 9.0 m, vertical wall height 2.30 m, curtain wall height 0.20 m, gable height 2.29 m, rafter length 5.05 m, eaves height 4.59 m, floor surface area 277.2 m^2, and volume 1010.4 m^3. The rafters were tilted at 27º from the horizontal plane to minimize the side effects of wind load that may blow over the roof of the greenhouse during winter months. At the same time it may be maximize the solar radiation flux incident on the roof of the greenhouse during that period due to decrease the solar incident angle. Moreover, with this inclined angle condensation will run down the underside rather than dropping from the cover, thus damaging crops and encouraging diseases will be minimized.

The greenhouse structural frame is formed of 38.1 mm hot dipped galvanized pipes (1.5-inch) with excellent anti-corrosion. The structural frame consisted of many parts (posts, beams, rafters, trusses) which easily assembled on the spot with joining parts and bolts and nuts, without any welding points to prevent damage the zinc coating on the material, which guarantee the optimal performance of anti-corrosion. It was covered with a single layer of fibreglass reinforced plastic (FRP) 1000 µm thick. The greenhouse was equipped with both forced water heating system supplied by 1500 litres hot water (heated by solar energy during daylight and biomass heating system just prior to sunset) and a complete evaporative cooling system (based on fan and pad system). It was also equipped with an environmental control board. The indoor air temperature during daylight-times was monitored using an ON-OFF controller to expel excessive heat at 26ºC and interrupt it at 25ºC. Thus, the fresh and cold air came from the evaporative cooling system was automatically drew by two extracting fans to pass through the longitudinal direction of the greenhouse when the indoor air temperature increased to 26ºC and the fans stopped when the air temperature reached to 25ºC.

2.2 Hybrid Heating System

2.2.1 Solar heating system

A solar water heater consists of six individual solar collector panels, each having a gross dimensions of 200 cm long, 100 cm wide, and 10 cm thick with net surface area of 2.0 m^2, and constructed from copper with a selectively absorbing surface coating as revealed in Fig. 1. The operating fluid (mix of water and antifreeze) was continuously passed through parallel waterways built into each panel. These 6 solar panels are arranged in two banks (upper and lower banks) with three panels in series in each bank. The upper and lower banks are in parallel array. The solar heating system is mounted on a movable frame outside the greenhouse so that to track the sun's rays from sunrise to sunset. It used a quadrant and clamp as a tilt angle controller. The movable frame is carried on an axial steel rod 127 mm diameter (5-inch) which connected to a large square reinforced concrete footing (3 m x 3 m x 0.30 m) for orientation of solar panels, where the movable frame is moved around the axial rod. Mains operating fluid entered the solar panels through a pressure reducing valve, a filter, and metering valve. A

vent pipe was positioned at the outlet from the panels to prevent damage in the event of boiling. The operating fluid was pumped to pass through the solar collector panels during daylight-times. After passing through the solar collector panels it was stored in a 1500 litres insulated storage tank situated inside the greenhouse in order to reduce the heat energy loss. The storage tank connected to the solar heating system by two junctions of insulated hot galvanized pipes 25.4 mm (1.0 inch) diameter. One junction is between the bottom of the storage tank and the bottom of the first solar panel in the lower bank (water inlet). The other junction is between the top of the storage tank and the last panel in the upper bank (water outlet). The flow rate of operating fluid through the solar collector panels (24 litres/min) was tested and adjusted each week using the control valve and a measuring cylinder with a stopwatch. The storage tank is connected to the biomass heat energy unit using solid fuel (wood of trees) to utilize the net heating value of wood for heating the operating fluid when the solar radiation was insufficient to raise the temperature into 95ºC.

Fig. 1. Solar collectors array, with a total surface area of 12.0 m^2 and mounted on a movable frame

2.2.2 Biomass heating system

The biomass burner was designed and constructed beside the greenhouse. Vertical biomass combustion equipment was used at which the biomass solid fuel (wood of tress) took place on horizontal stationary steel gate. The furnace design has been used as a stationary burning system with front-solid fuel burner. It was constructed in the form of modified Quonset shape (vertical walls with curved roof surface), and made of two layers of bricks, the inner is built of thermal red bricks (20 x 12 x 6 cm each) with gross dimensions of 2.0 m long, 2.0 m wide, and 2.5 m high. While, the outer layer is built of concrete blocks (40 x 20 x 20 cm) with gross dimensions of 2.10 m long, 2.10 m wide, and 2.65 m high, with 5 cm between the two layers. The gap between the two layers was fulfilled by loosely packed rock-wool insulation (k = 0.065 W/m ºC) in order to minimize the heat energy loss from the walls of biomass burner. In this way, the insulating performance and the thermal resistance may be enhanced.

A stainless steel coil (25.4 mm diameter and 36.0 m long) was used as a solution heat exchanger which horizontally located in central line of the biomass burner top section. The heat exchanger was connected to the storage tank located inside the greenhouse. One functional part of the heat energy generated from the combustion of the solid fuel was absorbed by the heat exchanger coil inside the biomass unit and transfers into the water passes through the coil. Another hot galvanized coil (50.8 mm diameter and 6.0 m long) was situated inside the biomass burner and functioned for heating outdoor air. The hot air was expelled into a perforated hot galvanized pipe (30.0 m long) located inside the greenhouse at a height of 2.35 m. Thus, the second functional part of the heat energy generated from the combustion of solid fuel was absorbed by the air passing through the hot galvanized coil. To provide and maintain an adequate amount of oxygen for igniting the solid fuel, the bottom section was connected to an air blower (2 hp) has two branches. One branch is functioned to provide the oxygen for igniting the solid fuel, and the other is used to pass the outdoor air into the hot galvanized coil located inside the biomass burner. The auxiliary heater (biomass burning system) switched ON just after the outlet water temperature of the solar heating system is equal to the water temperature of the storage tanks; also they switched ON when the water temperature in the storage tank was less than 95ºC. A schematic diagram and experimental set-up of the constructed hybrid experimental system is shown in Fig. 2. Sample of wood of trees was chemically analysed in the Chemical Department, Faculty of science, Cairo University. The chemical analysis is executed to determine the percentage of different elements contains in the wood of trees such as; Hydrogen (H), Organic carbon (C), Sulfur (S), Nitrogen (N), Oxygen (O), and Moisture content (MC). The chemical analysis of the sample is summarised and listed in Table 1. These percentages of

different elements contain in the wood was used to determine the gross heating value (higher heating value, HHV) and the net heating value (lower heating value, LHV).

2.3 Heat Energy Distributing System

To provide and maintain a given indoor air temperature regime on a particular site, heat energy consumption will vary with outdoor weather conditions, latitude, and proximity to the coast, elevation and exposure. Heat energy loss from the greenhouse is much higher than from modern conventional housing. This is due to the high rate of heat transfer through the light-transmitting cover, usually plastic or fiberglass. An overall heat transfer coefficient of 7.95 W/m^2 ºC is used for design calculations, and this is ten times greater than that for many modern housing [6]. Many factors contribute to heat energy loss (structure frame, covering materials, orientation, and heating systems) and it is essential that every possible method for reducing this loss be examined and where possible exploited.

To provide and maintain positively an indoor air temperature ranges from 18-19ºC, at nighttime during winter months, such as is required for sweet coloured pepper crop production and many other crops, the greenhouse was equipped with a complete solar heating system (six solar water heaters, storage tank, heat distributing system, and control board). To utilize the stored heat energy in the storage tank for heating indoor air inside the greenhouse, a heat exchanger with parallel flow system is constructed and installed inside the greenhouse. The system is mainly consisted of seven parallel rows of hot dipped galvanized pipes 38.1 mm diameter (1.5-inch) at an equidistance of 140 cm between two successive pipes, in order to provide adequate surface area of heat transfer. The total length of hot galvanized pipes inside the greenhouse is 230 m with total water volume of 262.2 litres. The heat exchanger (heat distributing system) is installed on the end of gable roof to be above the floor surface by 2.30 m. The hot operating fluid (heated by solar energy and biomass heat energy) from the insulated storage tank was pumped using thermal water pump (1.5 hp) to circulate through the heat exchanger when the indoor air temperature of the greenhouse is lowered to 18ºC. The indoor air temperature of the greenhouse at a height of 2.25 m above the

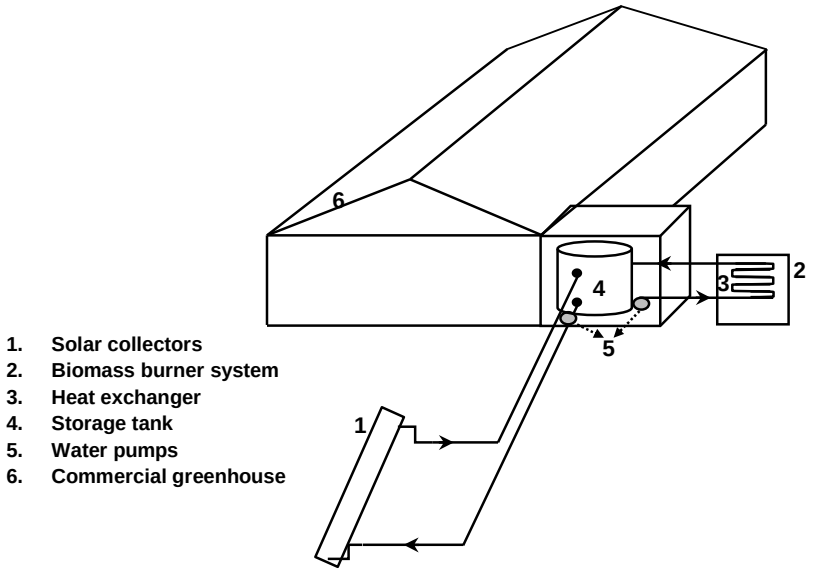

Fig. 2. Schematic diagram of the hybrid heat energy system using biomass heat energy system to assist solar heating system

Table 1. Chemical analysis of wood uses as a source of renewable energy

Solid fuel	H %	C %	S %	N %	O %	MC %
Wood of trees	5.68	52.10	0.01	0.25	42.64	12.65

floor level at night-times was also monitored using an ON-OFF controller (differential thermostat) to initiate heating at 18ºC and interrupt it at 19ºC. Therefore, the heated water from the insulated water storage tank was automatically pumped through an environmental control board to allow hot water circulates through the heat exchanger when the indoor air temperature of the greenhouse was lowered to 18^{o}C and stopped when the air temperature reached to 19ºC. More heat energy was continuously gained from the heat exchanger pipes during the heating cycle and cooling down stages.

2.4 Plant Cultivars

2.4.1 Germination of sweet coloured pepper seeds

A nursery of 8.0 m long, 4.0 m wide, and 3.0 m high was disinfected on 15th of July 2015. Soil mix-media for germinating sweet colours pepper (red and yellow colours) consisted of one bag of peat-moss and five bags of vermiculite was used. The peat-moss bag (volume of 0.3 m^3 and 60 kg weigh) was manipulated and enriched by adding little amount of chemical fertilisers (75 g of Rizolex-T 50% as a disinfectant substance, 500 g NPK fertiliser 19-19-19, 150 g of super phosphate, 100 g of potassium sulphate, and 75 g of iron as an enriched materials). Forty eight vegetative trays (84 growth blocks) were used to germinate the seeds of sweet coloured pepper. The tray blocks were full by soil mix-media and 1000 seeds (Marqueza, cv. And Tirza, cv., Enza Zaden, Netherlands) were directly planted on 18th of July 2015 (the appropriate time for planting seeds during July, according to the Biodynamic Calendar). After one ten days the sweet pepper seedlings were raised in the vegetative trays with 96.5% germination ratio.

2.4.2 Transplanting of sweet coloured pepper seedlings

The floor surface area inside the greenhouse was divided into 6 wide piles (90 cm wide, 20 cm high, and 50 cm wide space between two successive piles). Two rows per pile were planted at plant length on an average of 8 cm and 4 true leaves number. Rows are 70 cm apart, with 50 cm between plants within row. Seven hundred and twenty selected seedlings (780 seedlings) of sweet coloured pepper seedlings were manually transplanted inside the greenhouse on 3rd of September 2015 (the appropriate time for transplanting during September, according to the Biodynamic Calendar) for a plant population density of 2.814 plant m^{-2}. The transplanting operation was executed in the late afternoon to minimize transplant shock. Humic acid (Granules) by the rate of 0.25 gram/liter was placed in each hole just prior to transplanting to provide and enhance the growth of root system and to guard against insect attack. Measurements on the plants were taken throughout the growth period (growth rate, flowering rate, fruit set rate, production rate).

2.5 Measurements and Data Acquisition Unit

Meteorological station (Vantage Pro 2, Davis, USA) located beside the greenhouse on a height of 5 m from the ground level is used to measure different macroclimate variables such as, the solar radiation flux incident on a horizontal surface (pyranometer), dry-bulb, wet-bulb, and dew-point air temperatures (ventilated thermistor), wind speed and its direction (cup anemometer and wind vane), air relative humidity (hygrometer) and rainfall amounts (rain collector). The amount of heat energy added to the water in the storage tank which situated inside the greenhouse from the solar heating system (during daylight) and the biomass burning system (prior to sunset), a 12 channel data-logger (Digi-sense scanning thermometer type), was also used for taking and storing reading from different sensors (thermocouple type K) mounted at twelve different locations. A solarimeter integrated to a computer based data-logger, mounted on a surface parallel to the plane of the solar collectors was functioned to measure the global solar radiation flux incident on the tilted surface of solar collectors. The following data were regularly measured and recorded during the experimental work with a time interval of 5 min; (a) water-antifreeze solution temperatures entering and leaving the solar heating system (flat plate solar collectors) by thermocouples mounted on the water-antifreeze solution inlet and outlet lines, (b) water-antifreeze solution temperatures entering and leaving the biomass burner heat exchanger by thermocouples mounted on the water-antifreeze solution inlet and outlet lines, (c) air temperature entering and leaving the air heat exchanger coil mounted on the top section of biomass burner by thermocouples mounted on the inlet and outlet lines, (d) flue gas at the beginning and end of the thin-walled tube and peripheral temperature of tube located inside the greenhouse by

thermocouples mounted on the inlet and outlet lines, (e) water-antifreeze solution in the storage tank by thermocouple mounted on the centre point of tank, and (f) solar radiation flux incident on the tilted surface of solar heating system using solarimeter device.

2.5.1 Burden of heating

The indoor air temperature of 18ºC generally meets the needs of most protected cropping. The outdoor temperature follows the Delta zone (Egypt) 30% winter design dry bulb temperature (4ºC) which means 70% of the time, the outdoor temperature in Delta area for the rest of time is higher than 4ºC [6]. Heating process of the greenhouse accounts for 30-35% of the total cost of production of most greenhouse crops, and any increase in the price of fuel has a large proportionate effect on costs [17]. The requirements for heating a greenhouse reside in the task of adding heat at the rate at which it is lost [18]. Heat energy loss from the greenhouse is much higher than from modern conventional housing. This is due to the high rate of heat transfer through the light-transmitting cover, usually plastic or fiberglass. An overall heat transfer coefficient of 7.95 W/m^2 ºC is used for design calculations, and this is ten times greater than that for many modern housing [6]. Many factors contribute to heat energy loss (structure frame, covering materials, orientation, and heating systems) and it is essential that every possible method for reducing this loss be examined and where possible exploited. The total heat losses from indoor to outdoor of the greenhouse can be computed from the following equation [6,19]:

$$Q_{Heat} = Q_{Loss} \ , \qquad Watt \qquad (1)$$

$$Q_{Loss} = Q_{CL} + Q_{inf} \ , \qquad Watt \qquad (2)$$

Where, Q_{CL}, is the combination heat losses by conduction, convection, and radiation through the concrete blocks and the glazing materials of the greenhouse. It can be estimated by the following equation:

$$Q_{CL} = \sum U_o \, A_C \, (T_{ai} - T_{ao}) \ , \qquad Watt \qquad (3)$$

Where, U_0, is the overall heat transfer coefficient in W m^{-2} ºC^{-1}, A_C, is the total surface area of covering material m^2 and, T_{ai} and T_{ao}, respectively, are the indoor and outdoor air temperatures in ºC. The heat loss due to cold air infiltration through the structure (Q_{inf}) of outdoor cold air can be divided into sensible and latent heat. The heat energy quantity associated with having to raise the temperature of outdoor infiltration cold air up to indoor air temperature is the sensible heat component (q_S). The heat energy quantity associated with net loss of moisture from the space is classified as the latent heat component (q_L). The heat energy required to warm outdoor air entering into the the greenhouse by infiltration to the indoor air temperature is given by [6] as follows:

$$Q_{inf} = q_s + q_L \ , \qquad Watt \qquad (4)$$

$$q_s = m_a \, C_{pa} \, (T_{ai} - T_{ao}) \ , \qquad Watt \qquad (5)$$

Where, m_a, is the mass flow rate of cold air in kg s^{-1} (m_a = M N_F/3600), M, is the greenhouse volume (m^3) x density of air (kg. m^{-3}), N_F, is the air infiltration rate for fiberglass cover is 1.25 h^{-1} and, C_{pa}, is the specific heat of air in J. kg^{-1} ℃$^{-1}$. When addition of moisture to the indoor air is required to maintain winter comfort conditions, it is necessary to determine the energy needed to evaporate an amount of water equivalent to what is lost by infiltration (latent heat component of infiltration heat loss). This heat energy may be calculated by

$$q_L = m_a \, h_{fg} \, (W_i - W_o) \ , \qquad Watt \qquad (6)$$

Where, h_{fg}, is the latent heat of vaporization of water in J kg^{-1}(2454 × 10^3 J kg^{-1}), W_i, is the humidity ratio of the greenhouse indoor air in kg / kg_{dair}, W_o, is the humidity ratio of the greenhouse outdoor air, kg/ kg_{dair}.

2.5.2 Useful solar energy

The instantaneous useful heat energy gained by solar heating system (Q_U) is computed by the following equation [11]:

$$Q_u = F_R \, A_C \left[R(\tau\alpha) - U_C \left(T_{fi} - T_{ao} \right) \right] = m \, C_P \left(T_{fo} - T_{fi} \right) , \quad Watt \qquad (7)$$

Where, F_R, is the heat removal factor, A_C, is the solar collectors surface area in m^2, R, is the solar radiation flux incident on the tilted surface of collectors in W m^{-2}, τα, is the optical efficiency, U_c, is the overall heat transfer coefficient in W m^{-2} ºC, T_{fi}, inlet temperature of the operating fluid in ºC, T_{ao}, is the outdoor air temperature in ºC, m, is the mass flow rate of operating fluid in kg s^{-1}, C_P, is the specific heat of operating fluid in J kg^{-1} ºC^{-1}, and, T_{fo}, is the outlet temperature of the operating fluid in ºC.

The instantaneous overall thermal efficiency of the solar heating system is calculated as follows [11]:

$$\eta_o = \frac{m\, C_P\, (T_{fo} - T_{fi})}{R\, A_C}\ x\ 100\ ,\ \%\qquad (8)$$

2.5.3 Biomass heat energy system

The percentages of different elements contain in the wood which listed in Table 1 were used to determine the gross heating value (higher heating value, HHV) and the net heating value (lower heating value, LHV) using the following equations [17,20,21]:

$$HHV\ = 123.89\ (H) + 34.16\ (C) + 19.07\ (S) + 6.28\ (N) - 9.85\ (O),\quad MJ/kg\ \ of\ wood\qquad (9)$$

$$LHV = HHV - 2.453(9H + MC),\quad MJ/kg\ of\ wood\qquad (10)$$

The gross and net heating values of wood of trees which computed using the above two equations, respectively, were 20.652 and 19.088 MJ/kg. A mathematical model describes the system of a biomass burner unit is set up with an active condensation unit located inside the greenhouse. Furthermore, formula for the energy balance on the biomass burner unit are presented and discussed as follows:

$$NHV = Q_W + Q_a + Q_{loss},\quad kWh\qquad (11)$$

Where, NHV, is the net heating value in kWh, Q_w, is the heat energy absorbed by the operating fluid passes through the heat exchanger located inside the burner in kWh, Q_a, is the heat energy absorbed by the air passes through the coil situated inside the burner in kWh, and, H_{loss}, is the sum of heat energy loss from flue gas and outer surface of the biomass burner unit in kWh.

The heat energy absorbed by the operating fluid passes through the heat exchanger coil inside the burner (Q_w) can be computed in terms of the mass flow rate of operating fluid (m_w) in kg s^{-1}, specific heat of fluid (C_p) in kJ kg^{-1} $ºC^{-1}$, and temperature difference between outlet (T_{wo}) and inlet (T_{wi}) of operating fluid in ºC as follows:

$$Q_W = m_W\, C_P\, (T_{WO} - T_{Wi})\ ,\quad kWh\qquad (12)$$

The heat energy absorbed by the cold air passes through the heat exchanger coil which situated inside the biomass burner (Q_a) can be estimated using the following formula:

$$Q_a = m_a\, C_{Pa}\, (T_{ha} - T_{ca})\ ,\quad kWh\qquad (13)$$

Where, m_a, is the mass flow rate of air in kg s^{-1}, C_{pa}, is the specific heat of air in kJ kg^{-1} $ºC^{-1}$, T_{ha}, is the outlet temperature of hot air in ºC and, T_{ca}, is the inlet temperature of cold air in ºC. The heat energy losses from the biomass burner (Q_{loss}) are the sum of heat energy loss from the unit due to radiation and convection loss which dependent upon the actual output and the air cooled wall factor [22,23] and the heat energy loss during the quench of flue gas in the treatment unit. Heat losses could also be due incomplete combustion, high moisture content in the solid fuel (biomass), ash content in the wood, and the inefficient burner design. Therefore, the heat losses from the biomass burner can be computed using the following equation:

$$Q_{loss} = U_{ob}\, A_b\, (T_{hai} - T_{ao}) + m_{fg}\, C_{pfg}\, T_{fgo},\quad kWh\qquad (14)$$

Where, U_{ob}, is the overall heat transfer coefficient in W m^{-2} $ºC^{-1}$, A_b, is the surface area of biomass burner in m^2, T_{hai}, is the air temperature inside the biomass burner in ºC and, T_{fgo}, is the temperature of outlet flue gas in ºC.

2.5.4 Thermal efficiency of biomass burner

The biomass burner thermal efficiency was computed as the ratio of heat energy output (heat energy absorbed by the operating fluid and air, and heat energy gained by thin-walled tube from the flue gas) to the heat energy input (net heating value of biomass). There are two methods to determine the burner efficiency [24,25]:

Input-output method

$$Burner\ efficiency = \frac{Heat\ energy\ gained\ (outlet)}{Net\ heating\ value\ of\ biomass}\ x\ 100,\ \%\qquad (15)$$

Heat loss method

$$Burner\ efficiency = 1 - \frac{Heat\ energy\ losses}{Net\ heating\ value\ of\ biomass}\ x\ 100\ \%\qquad (16)$$

The heat loss method is commonly used as one can identify the heat losses and increase the efficiency by improving the burner's characteristics. For example, the radiation and convection heat loss for a burner is dependent

upon the actual output heat energy and the air cooled wall factor. Therefore, the burner efficiency could be optimised by balancing the cooled wall structure and thereby the actual heat energy output. Heat energy loss could also be due to incomplete combustion, high moisture content in field residues, high ash content in solid fuel materials, inefficient burner design. For instance, combustion high moisture biomass materials require heat energy to evaporate water in the field residues. The radiation and convection heat losses from the biomass burner are dependent on the actual output energy and the air cooled wall factor. The mass (weight) of dry air required to supply a given quantity of oxygen is 4.32 times the mass (weight) of the oxygen [6]. Oxygen contained in the solid fuel, except that in ash, should be deducted from the amount of oxygen required, since this oxygen is already combined with fuel components. Also, water vapour is always present in atmospheric air, and when the mass (weight) of air to be supplied for combustion is calculated, allowance should be made for it. Theoretical combustion air, unit mass (weight) of dry air/unit mass (weight) of fuel can be computed as follows [6]:

$$Mass\ of\ air\ = 0.0144\ (8\ C + 24\ H + 3\ S - 3\ O) \quad (17)$$

Where, C, H, S, and O, respectively, are the mass (weight) percentages of carbon, hydrogen, sulfur, and oxygen in the solid fuel. The actual mass of air supplied into the burner per unit time (second) can be estimated as follows:

$$Mass\ of\ air\ = A_P\ v\ \rho,\ kg/s \quad (18)$$

Where, A_p, is the cross-section area of the pipe to be supplied air in m^2, v, is the air speed just leaving the pipe, m s^{-1}, ρ, is the density of air, kg m^{-3}. The biomass burner unit not used during April month due to the solar energy stored was sufficient to provide heat energy required for heating the indoor air and maintaining the indoor air temperature at the desired level.

2.6 Vapour Pressure Deficit (VPD)

Vapour pressure deficit (VPD) is a good indicator of plant heat stress during daylight-time plant injury by fungal pathogens at nighttime. The Vapour pressure deficit is the difference (deficit) between the amount of moisture in the air and how much moisture the air can hold when it is saturated. Therefore, vapour pressure deficit is a valuable way to measure the greenhouse climatic conditions. VPD can be used to evaluate the disease threat, condensation potential, and irrigation needs of a greenhouse crop. An important step toward disease management is to prevent conditions that promote disease. Condensation prevention is important, since greenhouse pathogens often require a water film on the plant to develop and infect. The air is saturated when it reaches maximum water holding capacity at a given temperature (also called the dew-point). Adding moisture to air beyond its holding capacity leads to deposition of liquid water somewhere in the system.

More water vapour in the air means greater water vapour pressure. When the air reaches maximum water vapour content, the vapour pressure is called the saturation vapour pressure (VP_{sat}), which is directly related to air temperature. Thus, the differences between the saturation vapour pressure and the actual air vapour pressure is the mathematical definition of vapour pressure deficit (VPD). Higher vapour pressure deficit (VPD ≥ 2.0 kPa) means that the air has a higher capacity of hold water stimulating water vapour transfer (transpiration) into the air in this low humidity condition and plant heat stress and water stress can be occurred. Lower vapour pressure deficit VPD ≤ 0.43 kPa), on the other hand, means the air is at or near saturation, so the air cannot accept moisture from a leaf in this high humidity conditions which provides a good medium for fungal growth and diseases [26]. To express the synergistic effects of the dry-bulb temperature (T_{db}) and relative humidity of the indoor air temperature during daylight-time and at nighttime, the vapour pressure deficit (VPD) of the indoor air is used and calculated according to the following equation [6]:

2.6.1 Saturation vapours pressure of the indoor air (VP_{sat})

$$VP_{sat} = exp\ (Z)/1000,\ kPA \quad (19)$$

$$Z = (C_1/T) + C_2 + C_3\ T + C_4\ T^2 + C_5\ T^3 + C_6\ ln\ T \quad (20)$$

Where:

C_1 = - 5.800 220 6 E +03
C_2 = 1.391 499 3 E +00
C_3 = - 4.864 023 9 E -02
C_4 = 4.176 476 8 E -05
C_5 = -1.445 209 3 E -08
C_6 = 6.545 967 3 E +00

T = dry-bulb temperature of the indoor air in Kelvin.

2.6.2 Vapour pressure deficit of the indoor air (VPD_{air})

The vapour pressure deficit at the actual indoor air relative humidity (RH) in decimal can be computed from the following formula:

$$VPD_{air} = VP_{sat}\,(1 - RH),\ kPa \quad (21)$$

The previous equations are functioned to compute the vapour pressure deficit using computer Excel-sheet software.

2.7 Watering Operation

Protected cropping requires an adequate supply of moisture for optimum growth and maximum productivity. By supplying an adequate but regulated amount of moisture, it is possible to control the growth and flowering of plants. Therefore, after cultivating operation, the plants of sweet coloured pepper inside the greenhouse were irrigated by one cubic meter of water during each watering operation through the dripping irrigation system to establish good root-to-soil contact. Two cubic meters of water were continuously supplied to the greenhouse per week. Irrigation performance indicators which include; Water Use Efficiency (WUE), and Annual Water Productivity (AWP) were computed throughout the growth and production periods of different crops as follows [27]:

$$WUE = \frac{Total\ value\ of\ crop\ productivity\ (kg)}{Total\ water\ consumption\ (m^3)},\quad kg/m^3 \quad (22)$$

$$AWP = \frac{Total\ value\ of\ marketing\ price\ (L.E.)}{Total\ water\ consumption\ (m^3)},\quad LE/m^3 \quad (23)$$

Data are statistically analysed using Excel program. Linear regression analysis is used to examine the relationship between several dependent and independent variables. Significance level of 0.05 is conventionally taken as the minimum level of significant. Though where higher levels of significance found these values are included in the text (0.01 and 0.001).

3. RESULTS AND DISCUSSION

The macroclimatic conditions of the region are the prime parameter that affects growth rate and productivity of protected cropping and economics of the greenhouse productivity. A large burden of heating is essential requirement for greenhouse heating and relatively high prices of fossil fuels and their environmental impact, alternative heat energy sources for greenhouse heating has been gained utmost interest. The alternative sources of heat energy are the solar thermal energy storage systems (STES), and the thermal energy applications in space heating and hot water utilities of the modern biomass combustion system (BCS) could meet the contemporary heat energy requirements with the least possible environmental impacts.

3.1 Thermal Performance of Solar Heating System

The obtained results from the experimental work over the heating period from 3rd of November 2015 to 30th of April 2016 were evaluated to determine the thermal performance characteristics of the hybrid system. The solar heating system (six solar collectors, storage tank, heat distributing system, and control board) have been operating satisfactorily for almost six months without malfunction. Operating fluid temperatures have been monitored for six months from the beginning of November 2015. The monthly average solar energy contribution is plotted in Fig. 3. During the heating period, there were 1310 hours of bright sunshine of which 1109 hours (84.66%) were recorded and used in the thermal performance analysis and applications, slightly lower than average due to clouds. Although on day to day figures the correlation between sunshine hours and solar energy collected was lower, nevertheless the agreement was good on a monthly average basis as shown in Fig. 4. The monthly average heat energy gained (Q_u) was plotted against bright sun shine hours (N_S) as revealed in Fig 4. Regression analysis revealed a highly significant linear relationship (r = 0.9876) between the monthly average heat energy gained and the bright sunshine hour. The regression equation obtained was:

$$Q_u = 25.578 + 5.0134\,(N_s) \quad (24)$$

The discrepancies between months arise due to number of bright sunshine hours, solar altitude angles, operating fluid temperature in the storage tank at the beginning of each day, and number of operating hours. The y-intercept refers to the heat energy remained from the heating operation.

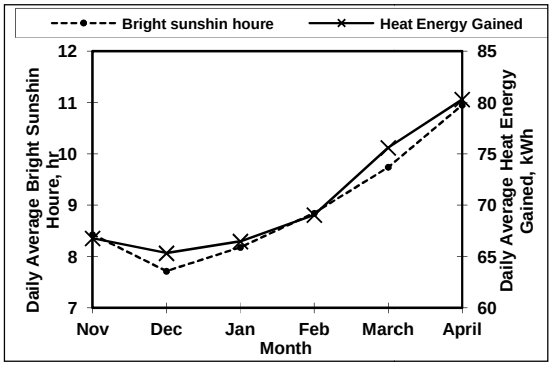

Fig. 3. Daily average solar energy collected by solar collectors and daily average sunshine hours during the experimental period

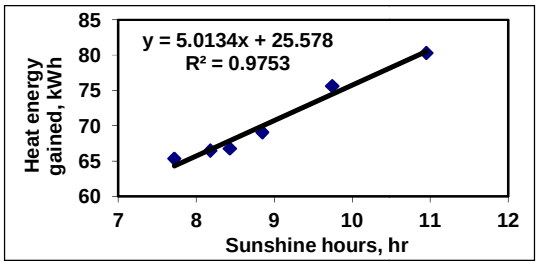

Fig. 4. Daily average heat energy gained against daily average bright sunshine hour

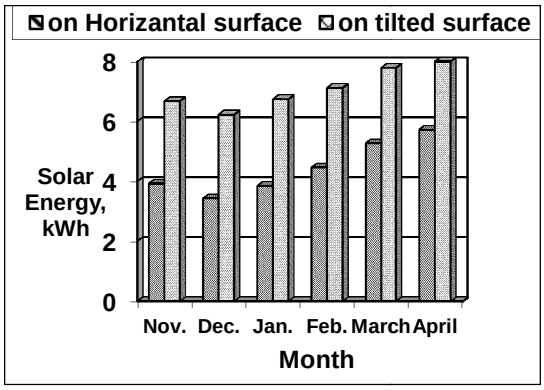

Fig. 5. Daily average solar radiation flux incident from sunrise to sunset on the horizontal and tilted surfaces

The actual solar radiation recorded on the tilted surface of solar collectors was always higher than that on the horizontal surface. For the duration of heating period (from November to April) the daily average solar radiation flux incident from sunrise to sunset on the horizontal and tilted surfaces is plotted in Fig. 5, consequently, the solar collector orientated and tilted from the horizontal plan increased the actual received solar radiation during that period by 1.701, 1.816 1.753, 1.595, 1.478, and 1.397, respectively. Under clear sky conditions, the solar energy available, absorbed solar energy, useful heat gain to storage, overall thermal efficiency, and solar energy stored in the storage tank increased gradually with solar time from sunrise to sunset till they attained the maximum values at noon. They then declined until reached the minimum values prior to sunset. The thermal performance analysis of the solar heating system is mainly assessed by its overall thermal efficiency in converting solar energy into stored heat energy. The solar energy available (Q), solar energy collected (Q_u), and solar energy stored (Q_s) are plotted in Fig. 6.

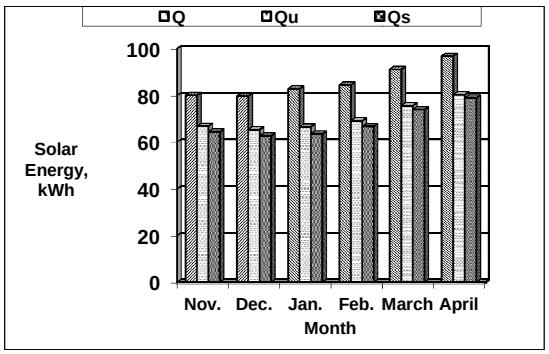

Fig. 6. Daily average solar energy available (Q), collected (Q_u), and stored (Q_s) during the heating period

They were obvious differences in solar energy available for the days recorded during the heating period. These differences in solar energy available can be attributed to the effect of the atmospheric conditions during the heating period and change in the solar altitude angles from month to another. The daily average absorbed solar energy during the heating period from November to April, respectively, was 74.573, 69.568, 75.288, 79.511, 87.030, and 89.342 kWh. The previous obtained data evidently showed that, the absorbed solar energy depends upon the optical efficiency (τα) of the solar collector, which is the product of effective transmittance of the thermal clear glass cover (0.95) and effective absorptance of the selective black absorber plate (0.98). These two factors depend strongly on the angle of solar incidence. Once each half an hour from sunrise to sunset, the sun's rays were perpendicular to the solar collector surface that tracked the sun's rays. Therefore, the solar incident angles at those

times were set at zero and the optical efficiency was at the maximum value (0.931). The daily averages absorbed solar energy converted into useful heat gain to storage depends strongly upon the heat removal factor. Heat removal factor depends on three important parameters; the collector flow factor, the panel efficiency factor, and the temperatures difference between the operating fluid and the absorber plate. The daily averages absorbed solar energy converted into useful heat gain to storage during the heating season from November to April, respectively, were 66.774, 65.337, 66.486, 69.062, 75.608, and 80.304 kWh/day. Mathematical analysis of the measured data showed that, during early and prior to sunset when the available solar radiation was less than 500 Watt and at the same times, the ambient air temperature was less than the operating fluid; little useful heat energy was acquired when the operating fluid passed through the solar collectors.

A comparison between the daily average total solar radiation available and total solar energy collected was executed. The solar energy collected (Q_u) was plotted against the solar radiation available (Q) as illustrated in Fig. 7. Regression analysis showed a highly significant linear relationship (r = 0.9824) between these parameters. The regression equation for the best fit was:

$$Q_u = 0.8228\ (Q) \qquad (25)$$

The regression equation revealed that the slope is equal to the daily average overall thermal efficiency of the solar heating system (82.28%). It also showed that the correlation between the solar energy collected (70.622 kWh) and the solar radiation available (85.110 kWh) was high except that the solar collectors appear to be more efficient in November, March, and April than in other months because the heat energy stored from the solar heating system during daylight was consumed at night-times (biomass heating system operated some days during November and March, and did not operated in April month). Accordingly the operating fluid temperatures in the storage tank at the beginning of each day throughout the three months were lower than the indoor air temperature and at the same time the intensity of solar radiation was high during these months. As the temperature difference between the absorber surface and the operating fluid passing through the solar collectors are increased, the heat transfer rate between the absorber surface and the solution is increased.

The overall thermal efficiency is the ratio of the useful heat energy gained by the operating fluid leaving the solar collectors to the solar energy available. The daily averages overall thermal efficiency of the solar heating system during the heating period from November to April, respectively, were 83.40%, 82.00%, 80.30%, 81.78%, 82.91% and 82.91%, consequently, 16.60%, 18.00%, 19.70%, 18.22, 17.09%, and

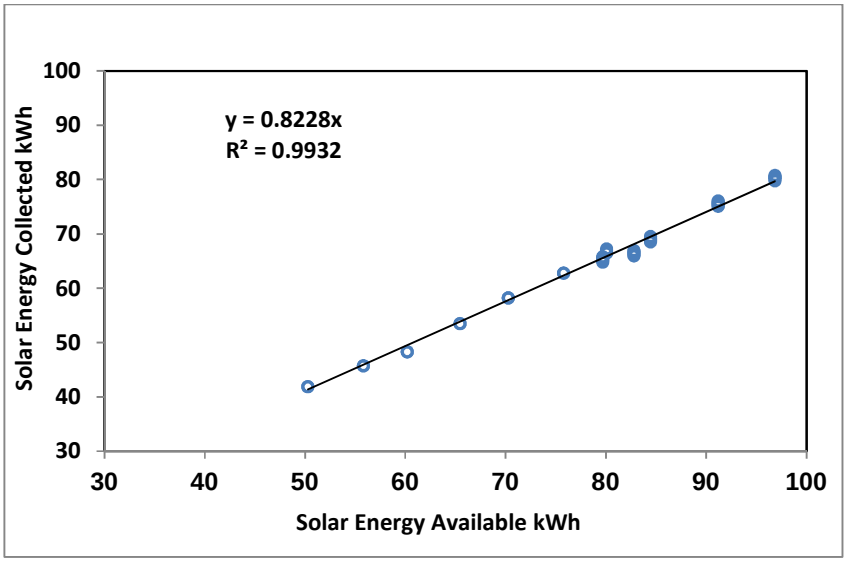

Fig. 7. Solar energy collected against solar energy available

Table 2. Nightly average outdoor air temperature, total heat energy lost, heat energy acquired from the solar and biomass heating systems, and the heat energy supplied from the storage tanks during the winter

	T_{ao}, ºC	Q_{loss}, kWh	Q_{stored}, kWh	$Q_{biomass}$, kWh	$Q_{supplied}$, kWh
Nov.	15.1	147.712	64.419	79.903	144.322
SD	1.7	85.867	28.190	22.975	27.855
Dec.	13.2	217.939	62.678	148.676	211.354
SD	1.2	61.495	26.428	47.488	38.985
Jan.	11.0	294.138	63.507	220.345	283.852
SD	1.8	94.583	30.778	15.387	25.803
Feb.	14.0	196.459	66.672	124.907	191.579
SD	2.6	117.493	29.357	21.287	27.352
March	14.8	162.802	73.922	85.490	159.412
SD	2.2	81.546	26.184	10.387	20.857
April	16.6	53.954	78.841	-	55.831
SD	2.3	23.835	24.550		18.733
Total	**84.7**	**1073.004**	**410.039**	**659.321**	**1046.350**
Mean	**14.1**	**178.834**	**68.340**	**131.964**	**174.392**
SD	**1.9**	**89.380**	**4.546**	**61.565**	**84.895**

17.09% of the solar energy available was lost. Heat transfer efficiency depends on the operating temperature of the absorber surface and the water inlet temperature. As the solution inlet temperature increased, firstly; the operating temperature of the absorber surface increased above the ambient air temperature and heat energy losses are thus increased, secondly; the difference in temperature between the absorber surface and the solution is reduced, making the heat transfer less efficient. Due to the overall thermal efficiency of the solar heating system is a combination of optical efficiency and heat removal factor; if one or both efficiencies increased the overall thermal efficiency is increased and solar collector thermal efficiency is thus increased. These data are in agreement with the data published by [6,11,28]. The daily averages solar energy stored in the storage tank during the heating period were 68.340 kWh (246.024 MJ), which gave an average storage system efficiency of 96.79% as listed in Table 2 above. Consequently, about 3.21% of the useful heat energy gained was lost.

3.2 Total Renewable Heat Energy Consumed During Winter Season

One of the objectives of this research work was to comprise the relationship between the heat energy supplied into the greenhouse and the heat energy lost from the greenhouse at nighttime during the heating season. The principal effect of greenhouses glazing material is to provide thermal resistance that reduces the overall rate of heat transfer into the surroundings. Greenhouse heating is an essential requirement for proper growth, development, and productivity of sweet coloured pepper crop. Since heating of a greenhouse is resided in the task of adding heat at the rate at which it is lost [18].

3.2.1 Heat energy losses from the greenhouse

The heat energy losses from the greenhouse were computed during the heating season. Most undesirable heat loss from a greenhouse occurs by long-wave radiation, conduction and convection (Q_c), and by infiltration (Q_{inf}). Greenhouse heat loss by infiltration of cold air was calculated by considering that the total exchange will be the sum of the sensible and latent heat energy exchange. The nightly average outdoor air temperature (T_{ao}), heat energy lost form the greenhouse (Q_{loss}), heat energy stored from the solar heating system (Q_{stored}), net heating value of the wood (NHV), and the heat energy supplied from the storage tank ($Q_{supplied}$) for heating indoor air of the greenhouse is listed in Table 2. The nightly average outdoor air temperature during the heating season was 14.1ºC, therefore, the heat losses from the greenhouse were 178.834 kWh (643.802 MJ). They varied from night to night and month to another according to the air temperature difference between indoor and outdoor. The highest values of nightly average heat losses from the greenhouse (294.138 kWh) occurred during January month, when the nightly average indoor and outdoor air temperatures

was 18.2 and 11.0ºC, respectively. Whilst, the lowest heat energy lost from the greenhouse (53.954 kWh) occurred during April month when the indoor and outdoor air temperatures, respectively, was 19.4 and 16.6ºC.

3.2.2 Heat energy gained from the biomass heating system

The nightly average weight of solid fuel used for heating the greenhouse varied from night to night, month to another and during the heating period. These variations were observed during the operating period of biomass burner from November 2015 till March 2016 which occurred according to the heat energy difference between the heat energy required for heating the greenhouse and solar energy stored in the storage tank. The nightly average weight of the solid fuel (wood of trees) from November to March was 31.376 kg. Therefore, about 4750.714 kg (4.751 ton) of solid fuel was used during the operating period of biomass heating system. The highest quantity of nightly average weight of solid fuel (53.829 kg) consumed during January month, whilst, the lowest quantity (18.442 kg) was consumed during November month. These quantity of solid fuel were combusted in a firebox inside the biomass burning system and provided nightly average net heating values of 166.695 kWh (600.102 MJ) as listed in Table 3. Operating fluid was pumped from the storage tank into the heat exchanger inside the biomass burner at which it was heated and delivered its heat energy into the operating fluid in storage tank, and then re-circulated through the heat exchanger. The fluctuations in heat energy acquired during the operating period as a function of time for each month during the heating period were observed. The nightly average net heating value (NHV), heat energy gained by the operating fluid (Q_w), the air (Q_a), total heat energy acquired (Q_{total}), and heat energy lost (Q_{loss}) from the biomass heating system during the operating period are listed in Table 3. The heat energy gained by the operating fluid and air at nighttime during the heating period from November to March varied from hour to hour and night to another. These variations in heat energy acquired due to feeding operations time. After each feeding of solid fuel into the biomass burner, greater value of net heat energy was achieved caused in increasing the heat energy gained by operating fluid.

For the duration of operating period of biomass burner, the nightly average heat energy gained by the operating fluid (Q_w) and added to the storage tank inside the greenhouse was 81.159 kWh (292.172 MJ). The fluctuations in heat energy acquired during the operating period as a function of time for each month during the heating period were plotted in Fig. 8. Cold outdoor air was brought into the coil of air heat exchanger at which it heated up and directly delivered its heat energy into the indoor air of the greenhouse through perforated water galvanized pipe. The outlet temperature of air blowing through blower-coil unit was allows higher than outlet operating fluid temperatures particularly during the feeding times of burner by the biomass solid fuels, due to the lower inlet air temperatures (ambient air) and higher values of net heating. However, the outlet air temperature was drastically decreased particularly in early morning, owing to quench of fire inside the biomass burner. For the duration of operating period of biomass burner, the nightly average heat energy gained by the air and added to the indoor air of the greenhouse (Q_a) was 50.705 kWh (182.538 MJ). There were fluctuations in the heat energy acquired by the air during the operating period. These variations in the heat energy gained by the air also due to feeding operations time. During the operating period of biomass burner, the nightly average heat energy gained by the operating fluid and air (Q_{total}) and added to the storage tank and indoor air of the greenhouse was 131.964 kWh (475.070 MJ). The remainder of heat energy generated from the biomass solid fuel was lost from the flue gas and biomass burner surface area. The nightly average heat energy lost from the flue gas and biomass burner surface area during the operating period was 34.831 kWh (125.392 MJ). The higher heat energy lost occurred during January month (65.637 kWh) due to the biomass solid fuels were absorbed moisture from the heavy rainfall (higher moisture content) during this month. Accordingly, incomplete combustion of the solid fuel usually occurred during this month. The cost analysis of the biomass heating system revealed that, the cost of solid fuel (wood, 31.376 kg/night) was 11.9 LE/night, based on the price of one ton is 380 LE. The nightly average total heat energy gained of biomass heating system is 177.4 LE according to the price of 1 kWh of electric energy in Egypt is 0.89 LE. While, the cost of heat energy lost from the biomass system is 31.0 LE. Consequently, the biomass heating system was economically employed for heating the greenhouse sweet coloured pepper under Egyptian conditions.

Table 3. Nightly average heat energy input (net heating value), heat energy output, heat energy lost, and thermal efficiency during the operating period

Month	Solid fuel, kg	Input heat energy, kWh	Output heat energy gained, kWh			Heat energy lost, kWh	Thermal efficiency, %
			Q_w	Q_a	Q_{total}	Q_{loss}	η
Nov.	18.442	97.978	51.078	28.825	79.903	18.075	81.55
SD	6.777	73.696	14.574	8.400	22.975	7.158	1.72
Dec.	34.736	184.545	91.965	56.711	148.676	35.869	80.56
SD	9.897	52.779	30.802	19.418	47.488	8.985	1.65
Jan.	53.829	285.982	132.123	88.222	220.345	65.637	77.05
SD	18.809	81.177	16.907	14.857	30.036	15.380	2.22
Feb.	29.829	158.066	77.266	47.641	124.907	33.159	79.02
SD	8.103	85.714	12.956	7.568	12,956	7.253	2.18
March	20.122	106.904	53.365	32.125	85.490	21.414	79.97
SD	5.706	69.988	6.496	3.918	10.494	4.577	1.37
Total	**156.881**	**833.475**	**405.797**	**253.524**	**659.321**	**174.154**	**-**
Mean	**31.376**	**166.695**	**81.159**	**50.705**	**131.964**	**34.831**	**79.63**
SD	**14.248**	**75.696**	**21.790**	**25.603**	**61.565**	**19.960**	**1.72**

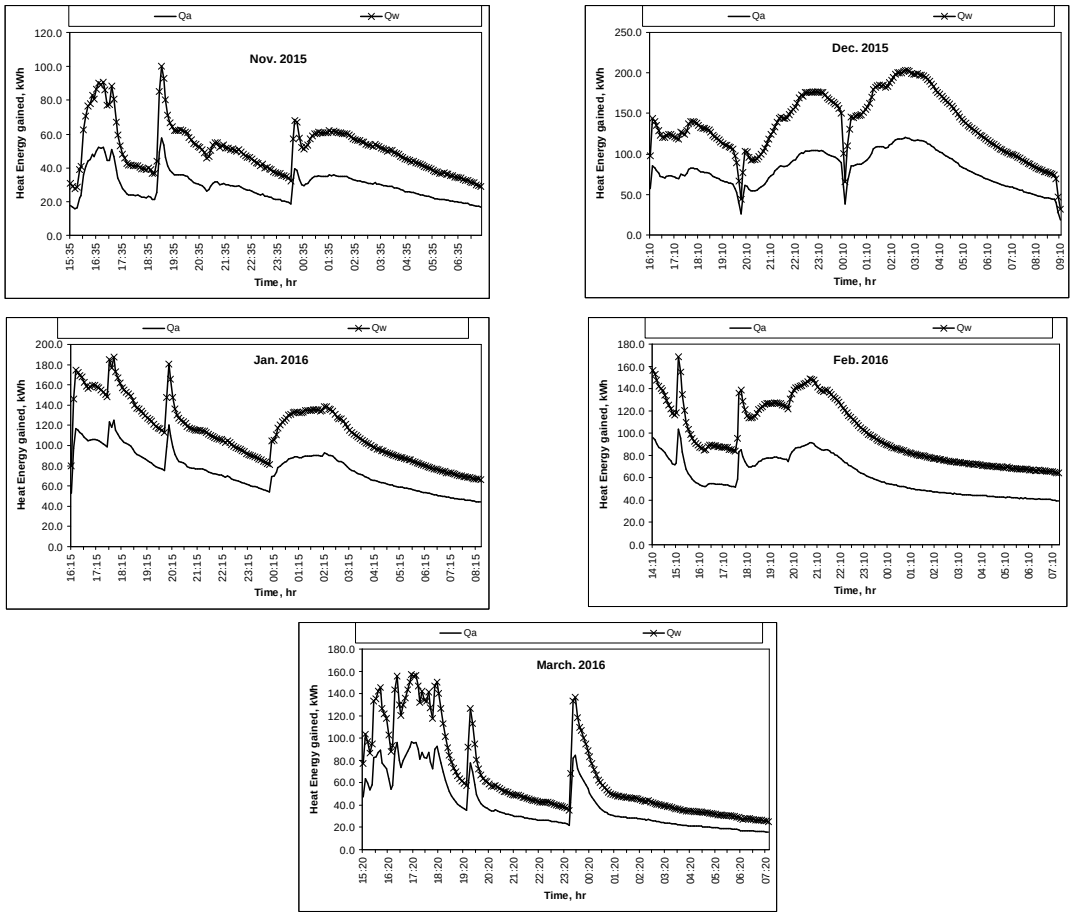

Fig. 8. Heat energy gained by the biomass heating system as a function of operating time from November to March

The actual obtained data of the heat energy balance on biomass unit revealed that, during the heating period, the heat energy absorbed by operating fluid represents 52.13%, 49.83%, 46.20%, 48.88%, and 49.92% of the total heat energy input, respectively. It also showed that, the heat energy gained by air during the same period represents 29.42%, 30.73%, 30.85%, 30.14%, and 30.05% of the total heat energy input, respectively. The heat energy balance also indicated that, the heat energy lost from the flue gas and biomass burner surface area during the operating period, respectively, represents 18.45%, 19.44%, 22.95%, 20.98%, and 20.03%. The measured heat energy gained (Q_{mg}) was plotted against predicted heat energy (Q_{pg}) as shown in Fig. 9. Regression analysis revealed a highly significant linear relationship (r = 0.9894) between these parameters. The regression equation obtained was:

$$Q_{mg} = 0.9241\ (Q_{pg}) \quad (26)$$

The relationship between the measured and predicted heat energy balance was highly agreement as the coefficient of determination was high (R^2 =0.979) The biomass burner efficiency could be optimized by balancing the cooled wall structure and thereby the actual heat energy output. The biomass burner thermal efficiency was computed as the ratio of heat energy output (heat energy absorbed by the operating fluid and cold air) to the heat energy input (net heating value of biomass) as mentioned previously.

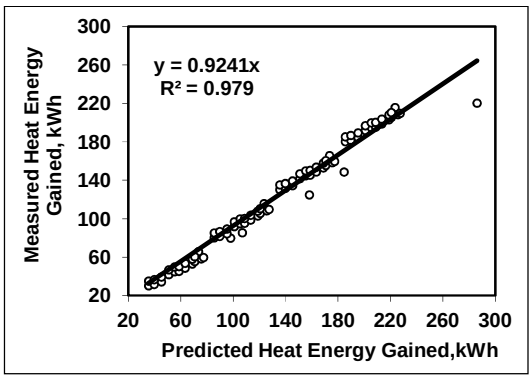

Fig. 9. Measured heat energy gained against predicted heat energy

Heat energy losses from the biomass burner could be due to incomplete combustion, high moisture content in the solid fuel, high ash content, inefficient biomass burner design, and heat energy includes in the exhaust smoke at the end. For instance, combusting of moistened biomass solid fuel requires heat energy to evaporate moisture in the fuel. Therefore, the thermal efficiency of biomass burner varied from night to night and month to another owing to the moisture content of the biomass solid fuel. For the duration of operating period of biomass heating system, the nightly average thermal efficiency was 79.63% as listed in Table 3. These data are in agreement with the data published by [20,29,30] when they reported that, the conventional small scale biomass burners reach only about 73 to 89% thermal efficiency based on the net heating value. The lowest thermal energy efficiency (77.05%) occurred in January month due to the solid fuel materials had higher moisture content from the rainfall during this month.

3.2.3 Heat energy providing

During the 180 days heating period, the solar heating system collected 12.712 MW of useful heat energy to storage of which 12.316 MW was stored in the storage tank and functioned for providing portion of total heat energy required for heating the greenhouses. The daily average heat energy provided by the hybrid renewable heat energy systems (biomass heating system assisted solar heating system) during the heating period is given in Table 4. It was compared with the total heat energy requirements for providing and maintaining the optimal level of indoor air temperature inside the greenhouse. During the heating season (from November 2015 to April 2016) the daily average useful solar energy collected was 70.622 kWh (254.239 MJ) of which 68.340 kWh (246.024 MJ) was stored in the storage tank and consumed during the growing season for heating the greenhouse. During the heating period, the storage tank inside the greenhouse was acquired 131.964 kWh (475.070 MJ) per night as supplementary heat energy from the biomass heating system. Thus, the hybrid heating system connected to the greenhouse provided 200.304 kWh (88.87%) of the daily total heat energy required (225.389 kWh). The daily average electrical energy consumed by the water pump which circulated the operating fluid between the solar heating system and the internal storage tank (Pump 1) was 4.250 kWh. The nightly average electrical energy consumed by the water pump (Pump 2) which circulated the operating fluid between the storage tank and the heat exchanger inside the biomass heating

Table 4. Daily average total heat energy normally required (kWh) for heating the greenhouse during the heating season (180 days)

Energy	Heat energy, kWh/day	Providing of total heat energy, %
Solar and biomass heat energies consumed		
Daily useful heat energy collected	70.622	31.33
Daily heat energy stored in the storage tank	68.340	30.32
Nightly heat energy gained from the biomass system	131.964	58.55
Total heat energy consumed per night	200.304	88.87
Electrical energy consumed		
Daily electrical energy used by water pump (1)	4.250	1.89
Nightly electrical energy used by water pump (2)	5.075	2.25
Nightly electrical energy used by water pump (3)	7.485	3.32
Nightly electrical energy used by air blower	8.275	3.67
Total electrical energy used during heating operation	25.085	11.13
Total energy actually used by greenhouse 1	**225.389**	**100.00**

system was 5.075 kWh. The nightly average electrical energy consumed by the water pump (Pump 3) used to distribute the stored heat energy in the storage tank within the greenhouse was 7.485 kWh. The air blower consumed electrical energy of 8.275 kWh per night. Therefore, the three different water pumps and the air blower consumed 25.085 kWh (11.13%) of electrical energy per night of nightly total heat energy required for heating the greenhouse.

The potential saving from solar power was not fully realized as compared with biomass heat energy for two main reasons: Firstly, little solar energy was collected in the first two hours after sunrise and the last prior to sunset due to low solar altitude angle and high operating fluid temperature in the storage tank. As the heat energy stored in the storage tank was not completely consumed at some nights, therefore at the beginning of some days more than two hours of sunshine were lost. Secondly, during the coldest month (January) the outdoor air temperature at some night-times was lowered to 4.8ºC for the majority of the last three hours of night-times (three hours prior to sunrise) resulting in great amount of heat energy loss. Accordingly, there was 220.345 kWh (793.242 MJ) of biomass heat energy were added into the operating fluid in the storage tank inside the greenhouse and the indoor air during this month. Therefore, a movable baffle was used to close the outside surface area of the cooling pads at the end of daylight to minimize the heat losses due to infiltration of cold air. In spite of these heat energy losses the hybrid system is providing a significant proportion of the total heat energy required for heating the greenhouse. If the electrical energy consumed by the water pumps and the air blower are ignored because of these units are a basic components of the renewable heat energy and does not a source of heat energy addition into the greenhouse, the proportions of heat energy provided using renewable sources of heat energy systems for heating the greenhouse is 100%. The cost analysis of the hybrid heating system revealed that, the nightly average total heat energy consumed was 200.304 kWh which equivalent to 178.3 LE, if the electric energy is functioned. While, the nightly fixed and variable costs of the hybrid system is 25.2 LE. Therefore, the hybrid heating system was economically operated for heating the greenhouse.

3.3 Effect of Heating Greenhouse on Microclimatic Conditions

Both long and short-term production related processes, such as photosynthesis, transpiration and reallocation assimilates, flowering and fruit setting, depend on microclimatic factors (solar radiation, air temperature, and air relative humidity during daylight and indoor air temperature and relative humidity at night), and in the case of greenhouse crop. The indoor air temperature of the greenhouse had compared with the outside air temperature as an important measure of the effectiveness of the environmental control system. The fluctuations of air temperature surrounding the crops play an important role for their growth rate, development, and productivity. Fluctuation changes in air temperature, caused by the ON-OFF control board, evidently observed inside the greenhouse.

A temperature gradient developed along the centerline of greenhouse and its value varied with time during each heating cycle. The nightly average outdoor and indoor air temperatures of the greenhouse, respectively, were 14.1 and 18.6ºC. The indoor air temperatures of the greenhouse which continuously heated using hybrid renewable energy systems during the winter months was always greater than that the outdoor air temperature by 4.5 and at the same time it was at and around the optimal level of air temperature (18-19ºC). The nightly averages minimum outdoor and indoor air temperatures recorded at 06.15 h (just prior to sunrise), respectively, were 7.2 and 17.7ºC. In combination with the low temperature requirements of the most commonly cultivated horticultural crops (minimum air temperatures for tomato, green bean, cucumber, and sweet pepper, respectively, are 13, 14, 15, and 16ºC according to [28,31,32]. During the heating season (six months) the heated greenhouse achieved a minimum air temperatures over the recommended minimum level (16ºC) by 1.7ºC, which provided the possibility of a good productivity for a limited cost.

Most protected cropping grow best within a fairly restricted range, typically 45% to 80% air relative humidity for many varieties [33]. High air relative humidity is the response of pathogenic organisms. Most pathogenic spores cannot germinate at indoor air relative humidity below 85%. Low air relative humidity increases the evaporative demand on the plant to the extent that moisture and water stresses can occur during daylight-time, even when there is an ample supply of water to the roots. The nightly average outdoor and indoor air relative humidity during the heating period was 80.6% and 65.4%, respectively. This means that at nighttime, the indoor air relative humidity was lower than that of the outdoor by about 15.2%. This variation can be attributed to the effectiveness of the heating system using biomass heating system assisted solar heating system for heating up the indoor air of the greenhouse. Indoor air relative humidity of the greenhouse during the growth period was at and around the optimal level. Cyclic changes were also observed in the indoor air relative humidity, and the humidity ratio, which measured inside the greenhouse. The cyclic variation in air relative humidity occurred at the peak of the heating cycle in the greenhouse. Thus, the indoor air relative humidity of the greenhouse was decreased by 5.1% after the peak of each heating cycle, whilst at the end of the cooling down it increased by 6.9%. Furthermore, stable microclimate conditions (air temperature and relative humidity) could reduce greenhouse heat losses and meet the physiological requirements for growth, development, and productivity of fresh sweet coloured pepper. At daylight times, the daily averages outdoor and indoor air relative humidity of the greenhouse was 52.7% and 56.8%. Due to the greenhouse is also equipped with a complete direct evaporative cooling system based on fan-pad system, the daily average indoor air relative humidity of the greenhouse was higher than that the optimal minimum level (45%, according to [33].

Vapour pressure deficit (VPD) is a good indicator of plant stress brought about by either excessive transpiration (higher VPD values ≥ 2.0 kPa) or the inability to transpire adequately (lower VPD values ≤ 0.43 kPa) as mentioned by [34]. Vapour pressure deficit relates to the customary thinking about indoor air relative humidity and air temperature. Higher vapour pressure deficit means that, the air surrounding the plant has a higher capacity to hold water, stimulating water vapour transfer (transpiration) into the air in this lower air relative humidity conditions. Lower vapour pressure deficit, on the other hand, means the plants are unable to evaporate enough water to enable the transport of minerals (such as calcium) to growing plant cell, even though the stomata may be fully open. The nightly average indoor vapour pressure deficit (VPD) of the adapted greenhouse during the heating period was 0.7337 kPa which was higher than the critical level (PVD ≤ 0.43 kPa). When the vapour pressure deficit is extremely low, water may condense out of the indoor air onto leaves, fruit, and other parts of plants. This can provide a good medium for fungal growth and pestiferous diseases. Whilst, the daily average indoor vapour pressure deficit of the greenhouse during the same period was 1.5547 kPa which was lower than the critical level (VPD ≥ 2.0 kPa) during daylight-time. The leaves temperatures closely correlated with the surrounding air temperature. Cyclic changes in both the leaves and the indoor air temperatures with a peak-to peak difference of 1.2 - 2.4℃ were observed during the heating period. Accordingly, the nightly average VPD at the plant leaves during the heating period was 0.0 kPa. However, the dew-point temperature of the air surrounding the stomatoes (20℃) was lower than the leaves temperature (20.4℃), thus, the moisture did not condensed on the leaves surface of the plants throughout the growth period.

3.4 Effect of Microclimatic Conditions on Productivity of Pepper

Due to the microclimatic conditions (indoor air temperature and air relative humidity) of the adapted greenhouse was at or around the optimal levels during daylight-time (using evaporative cooling system) and at nighttime (using hybrid heating system), optimal vegetative growth rate and productivity was achieved. This achievement may be attributed to the biochemical reaction rates of various metabolic processes, absorption rate of nutrient elements and water uptake by root system during different days of growth which strongly affected by the microclimatic conditions, particularly the indoor air temperature and relative humidity of greenhouse (G1). This is in agreement with the data published by [35,36]. The numbers of fruits being seated on the plants within the greenhouse was 9810 fruits. The number of fruits during the harvesting period ranged from 212 to 1585 fruits. The total fresh yield of sweet coloured pepper crop was 2388.823 kg with productivity rate of 8.618 kg/m^2. The fresh yield of sweet coloured pepper reached to the peak harvest (404.117 kg) on February month. The average weight of one fresh fruit harvested 243.509 g/fruit. The highest average weight of one fruit (314.642 g/fruit) was achieved from the first harvest. While, the lowest averages weight of one fruit (173.120 g/fruit) occurred during the last harvest.

The irrigation water use efficiency for the adapted greenhouse during the growing season was 29.860 kg/m^3. These data revealed that, the irrigation water use efficiency for the heated greenhouse was closest to the optimum value (30.3 kg/m^3) recommended by [25]. The total fresh yield of sweet coloured pepper produced from the greenhouse (2388.823 kg) with high quality of fresh fruits was sold by LE 35 832 (15 LE/kg) and provided an annual irrigation water productivity of 447.9 LE/m^3.

4. CONCLUSION

This paper has undertaken a study to carry out both solar and biomass heating systems for greenhouse heating during winter season of 2015-2016 at the eastern area of coastal delta, Egypt. Some concluding remarks from this research work are listed as follows:

- The solar heating system provided 68.340 kWh (30.32%) and the biomass heating system provided 131.964 kWh (58.55) of the nightly total heat energy required (225.389 kWh) for heating the greenhouse. Accordingly, the hybrid heating system provided 200.304 (88.87%) of the total heat energy required.
- Greenhouse heating provided and maintained an optimal level of microclimatic conditions (indoor air temperature and relative humidity) for sweet coloured pepper. Therefore, the nightly average vapour pressure deficit (0.7337 kPa) at night-times during the winter season was always higher than the critical level (PVD ≤ 0.43 kPa).
- High quantity and quality of fresh yield (8.618 kg/m^2) were achieved from this greenhouse. It also provided high water use efficiency of 29.860 kg/m^3. High water use efficiency (29.860 kg/m^3) and high annual irrigation water productivity (447.9 LE/m^3) were achieved during this study.

COMPETING INTERESTS

Authors have declared that no competing interests exist.

REFERENCES

1. Benli H. A performance comparison between a horizontal source and a vertical source heat pump systems for a greenhouse heating in the mild climate Elazig, Turkey. Applied Thermal Engineering. 2013;50:197–206.
2. Khosla S, Spieser H. Use of biomass for heating greenhouses in Ontaio-Rules and bast management practices. Fact-sheet, Order No. 08-015W, Ministry of Agriculture, Food and Rural Affairs, Ontario; 2008.
3. Vadiee A, Martin V. Energy management in horticultural application through the closed greenhouse concept, state of art. Renewable and Stainable Energy Reviews. 2012;16:5087–5100.
4. Sayigh AAW. Renewable energy: Global progress and examples. Renewable Energy, WREN. 2001;15–17.
5. Kalogirous S. The potential of solar industrial process heat applications. Applied Energy. 2003;76:337–361.
6. ASHRAE. Handbook of fundamentals. American Society of Heating, Refrigerating, and Air Conditioning Engineers, New York, USA; 2011.
7. Foster R, Ghassemi M, Cota A. Solar energy: Renewable energy and the

environment. First Edition, by Taylor and Francis Group, LLC, New York, USA; 2010.
8. Tripanagnostopoulos Y, Souliotis M, Nousia TH. 'Solar collectors with colored absorbers. Solar Energy. 2000;68:343–357.
9. Wazwaz J, Salmi H, Hallak R. Solar thermal performance of nickel-pigmented aluminium oxide selective absorber. Renewable Energy. 2002;27:277–292.
10. Orel ZC, Gunde MK, Hutchins MG. Spectrally selective solar absorbers in different non-black colours. Proceeding of WREC VII, Cologne on CD-ROM; 2002.
11. Duffie JA, Beckman WA. Solar engineering of thermal processes. Fourth Edition, John Wiley & Sons, Inc., Hoboken, New Jersey, USA; 2013.
12. Sipila K, Pursiheimo E, Savola T, Fogelholm C, Keppo L, Ahila P. Small-scal biomass CHP plant and district heating. VTT research notes 2301, Finland; 2008. Available:www.vtt.fi/inf/pdf/tiedotteet/2005/T2301.pdf
[Accessed 10. 02. 08]
13. Vamvuka D, Tsoutsos T. Energy exploitation of biomass residues in the island of Crete. Energy Exploration and Exploitation. 2002;20(1):113–120.
14. Vallios I, Tsoutsos T, Papdakis G. Design of biomass district heating systems. Biomass and Bioenergy. 2009;33:659–678.
15. Paengjuntuek W, Mungkalasiri J. 'Thermal efficiency evaluation of hydrogen production from biomass in Thailand. Thammasat International Journal of Science and Technology. 2013;18(4):37–43.
16. Peterseim JH, Tadros A, Hellwig U, White S. Increasing the effiency of parabolic trough plants using thermal oil through external superheating with biomass. Energy Conversion and Management. 2014;77:784–793.
17. Chau J, Sowlati T, Sokhansanj S, Preto F, Melin S, Bi X. Techno-economic analysis of wood biomass boilers for the greenhouse industry. Applied Energy. 2009a;86:364-371.
18. Nelson PV. Greenhouse operation and management. Fourth Edition, Prentice-Hall, Inc., New Jersey 07632;2006.
19. Esen M, Yuksel T. Experimental evaluation of using various renewable energy sources for heating greenhouse. Energy and Buildings. 2013;65:340-351.
20. Khor A, Ryu C, Yang Y, Sharifi VN, Swithenbank J. Straw combustion in a fixed bed combustor. Science Direct, Fuel. 2007;86:152-160.
21. Musil-Schlaeffer B, McCarry A, Haslinger W, Woergetter M. Standards and performance of residential biomass boilers in Europe. EM magazine, A&WMA: Air and Waste management Association; 2011.
22. DOE. Energy efficiency program for certain commercial and industrial equipment: Test procedures and efficiency standards for commercial packaged boilers. Docket No. EE-RM/TP-99-470, Washington, DC: Office of Energy Efficiency and Renewable Energy, Department of Energy; 2004.
23. Falconett I, Nagasaka K. Comparative analysis of support mechanisms for renewable energy technologies using probability distributions. Renewable Energy. 2009;35(2010):1135–1144.
24. Barroso J, Barreras F, Amaveda H, Lozano A. On the optimization of boiler efficiency using bagasse as fuel. Fuel. 2003;82(12):1451-1463.
25. Covarrubias CM, Romero CE. Burner performance evaluation using test code. J. Energy Engineering-ASCE. 2007;133(2): 78-81.
26. Pringer JJ, Ling PP. Greenhouse condensation control; Understanding and using vapour pressure deficit. Extension Fact-sheet, Ohio Sate University Extension, USA; 2004.
27. Lorite IJ, Mateos L, Federes. Evaluating irrigation performance in a Mediterranean environment, II variability among crops and farmers. Irrigation Science. 2004;23:85-92.
28. Wang Xuan, He Tao, Huang Heping. Solar heating and cooling application potential and application case analysis in new-type urbanization in China. Energy Procedia. 2014;48:1635-1641.
29. Louis-Martin D, Mark L. Biomass heating for improved greenhouse efficiency. Macdonald Reports, Bio-resource Engineering, McGill University, Macdonald Campus; 2010.
30. Hebenstreit B, Schnetzinger R, Ohnmacht R, Hoftberger E, Haslinger W. Efficiency optimization of biomass boilers by combined condensation – heat pump – system. Proceedings of ECOS 2011 Novi Sad, Serbia. 2011;1465-1477.

31. Spanomitsios GK. Temperature control and energy conservation in a plastic greenhouse. Journal of Agricultural Engineering Research. 2001;80(3):251-259.
32. Kittas C, Bartzanas T, Jaffrin A. Temperature gradients in a partially shaded large greenhouse equipped with evaporative cooling pads. Biosystems Engineering. 2003;85(1):87-94.
33. Öztürk HH, Başçetinçelik A. Effect of thermal screens on the microclimate and overall heat loss coefficient in plastic tunnel greenhouses. Turk J Agric. 2003;27: 123-134.
34. Argus Control System LTD. Understanding and using VPD. Canada V4B 3Y9; 2009. Available:www.agruscontrols.com
35. Özkan B, Ceylan RF, Kizilay H. Energy inputs and crop yield relationships in greenhouse winter crop tomato production. Renewable energy. 2011;36: 3217-3221.
36. Daniel JC, Vansickle JJ. Competitiveness of the Spanish and Dutch greenhouse industries with the Florida fresh vegetable industry. Horticultural Sciences Department, Florida Cooperative Extension Service, Institute of Food and Agricultural sciences, University of Florida; 2012.

Peer-review history:
The peer review history for this paper can be accessed here:
http://sciencedomain.org/review-history/16957